Organic LETTERS

Letter

pubs.acs.org/OrgLett

Seven-Membered Ring Nucleoside Analogues: Stereoselective Synthesis and Studies on Their Conformational Properties

Maryam Habibian,[†] Saúl Martínez-Montero,[†] Guillem Portella,[‡] Zhijie Chua,[†] D. Scott Bohle,[†] Modesto Orozco,[§,∥] and Masad J. Damha*[,†]

[†]Department of Chemistry, McGill University, 801 Sherbrooke Street West, Montreal, QC H3A 0B8, Canada

[‡]Chemistry Department, University of Cambridge, Lensfield Road, Cambridge CB2 1EW, U.K.

[§]Joint BSC-CRG-IRB Programme on Computational Biology, Institute for Research in Biomedicine, Baldiri i Reixac 19, 08028 Barcelona, Spain

[∥]Departament de Bioquímica i Biologia Molecular, Facultat de Biologia, Universitat de Barcelona, Avgda Diagonal 643, 08028 Barcelona, Spain

Supporting Information

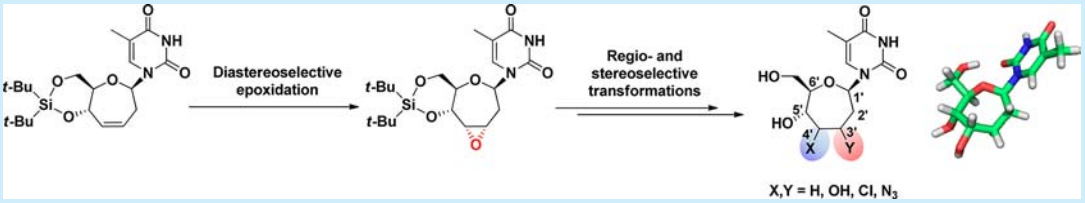

ABSTRACT: The synthesis of a novel series of seven-membered ring nucleoside analogues as candidates for biological screening and gene silencing applications is described. The key step in the synthetic approach is a stereoselective synthesis of an epoxide that is used as a common synthetic intermediate to prepare functionalized oxepane nucleoside derivatives. The conformational landscape and preferred ring-puckering of selected oxepane nucleosides was also studied by NMR, X-ray crystallography, and quantum mechanical calculations.

Nucleoside analogues are extremely valuable compounds in medicinal chemistry.[1,2] Modification of the furanose moiety and its impact on the conformation and biological activity of nucleosides has been studied extensively.[3,4] Due to their more challenging accessibility, ring-expanded derivatives have been considerably less explored. Hexose- and hexitol-based nucleosides are the most studied among this class and were first described by the Eschenmoser[5,6] and Herdewijn[7,8] groups, respectively. In the hexitol series (**1**), the flexible furanose ring is replaced with a more rigid six-membered sugar ring, and the position of the nucleobase is moved from the anomeric carbon to the 3′-position (Figure 1). Nucleic acids derived from hexitol nucleosides have been proven useful for gene silencing, biotechnology, and synthetic biology applications.[9]

Seven-membered oxepane scaffolds are commonly found in natural products and biologically active molecules.[10−13] In the search for ring-expanded DNA analogues, we recently reported the synthesis of oligonucleotides constructed from oxepane nucleosides (oxepane nucleic acids, ONA, **2**).[14] It was hypothesized that expanding the carbohydrate moiety of DNA to a seven-membered skeleton would provide conformationally more flexible sugars relative to the six-membered ring pyranose, thus better mimicking the conformation of natural 2-deoxyribose. Indeed, ONA, like DNA oligonucleotides, are able to trigger RNase H-mediated degradation of a complementary RNA strand.[14] Following our work, a few more

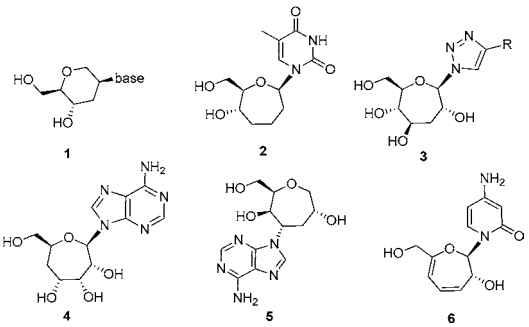

Figure 1. Hexitol nucleosides (**1**), oxepane nucleoside previously synthesized in our laboratory (**2**), other examples of oxepane nucleosides reported to date (**3**-**6**).

examples of oxepane nucleoside analogues have been reported as potential glycosidase inhibitors (**3**),[15] antiviral agents (**4**[16] and **5**[17]), and unexpected byproducts of nucleoside syntheses (**6**)[18] (Figure 1).

As part of our ongoing interest in the development of nucleosides with expanded sugar rings,[14,19] we herein describe the synthesis of several novel oxepane-based nucleosides that are excellent candidates for biological screening and building blocks

Received: September 24, 2015
Published: October 22, 2015

DOI: 10.1021/acs.orglett.5b02769
Org. Lett. 2015, 17, 5416−5419

for gene silencing oligonucleotides.[20] The focus of this study is to use a common and versatile chiral synthetic intermediate to generate structurally diverse oxepane nucleosides.

We also report for the first time on the conformation of some of the synthesized analogues, assessed by X-ray crystallography, NMR, and theoretical (classical and quantum mechanical) calculations.

Synthesis and Characterization of Oxepane Nucleosides

An efficient five-step synthesis of oxepene **7** was previously described by our laboratory,[14] starting from commercially available tri-*O*-acetyl-D-glucal and adapting the ring expansion strategy described by Hoberg et al.[21] The attractiveness of **7** is that its alkene functionality can be manipulated for the introduction of different functional groups in the seven-membered ring. For example, access to a new series of functionalized oxepane nucleoside monomers was devised from an asymmetric epoxidation of **7**, enabling the diastereoselective installation of new stereocenters. Thus, we first focused on finding the best conditions for the stereoselective epoxidation of **7** (Scheme 1).

Scheme 1. Stereoselective Synthesis of Oxepane Nucleoside 8

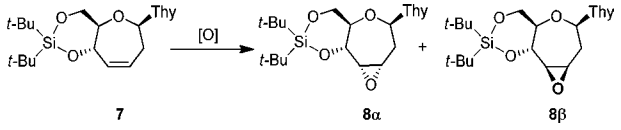

We attempted to take advantage of the allylic alcohol to perform an asymmetric epoxidation. Thus, the silyl bridge of **7** was cleaved before subjecting it to epoxidation with $VO(acac)_2$.[22] Under the experimental conditions, we observed rapid decomposition of the starting material. Classical oxidation of **7** with *m*CPBA in DCM afforded a 2:1 α/β diastereomeric mixture of the epoxide in 50% yield. The two isomers showed very similar polarity (TLC, $\Delta R_f < 0.1$), making it difficult to separate them by silica gel column chromatography (Table 1, entry 1). Next, we used a chiral catalyst to induce stereoselectivity. Jacobsen catalyst is an attractive candidate due to its ability to catalyze stereoselective epoxidations of unfunctionalized olefins. When **7** was treated with 5 mol % of (*S*,*S*)-Jacobsen catalyst in a $NaOCl/CH_2Cl_2$ biphasic system and in the presence of pyridine *N*-oxide, a 1:1.7 α/β diastereomeric mixture was obtained (Table 1, entry 2). A significant improvement in stereoselectivity (87% de) was observed when the same reaction was carried out with the (*R*,*R*)-Jacobsen catalyst under the same conditions (Table 1, entry 3). The reaction proceeded in better yields (58%) by increasing the catalyst loading to 10 mol % without any decrease in stereoselectivity (Table 1, entry 4). Traces of **8β** were removed by flash column chromatography. It is noteworthy that, at this stage, the configuration of the epoxide ring was ambiguous as the NOESY NMR spectra did not show the expected key correlations. However, subsequent formation of the anhydro oxepane **12** from **8α** (Scheme 3) allowed the assignment of stereochemistry at C3′−C4′.

Table 1. Epoxidation of Protected Oxepene 7 under Different Conditions

entry	epoxidation reagent	cat. (mol %)	yield (%)	**8α**/**8β**[f]	de (%)
1[a]	*m*CPBA		50[d]	2:1	33
2[b]	(*S*,*S*)-Jacobsen cat.	5	36[d]	1:1.7	26
3[b]	(*R*,*R*)-Jacobsen cat.	5	34[e]	14:1	87
4[c]	(*R*,*R*)-Jacobsen cat.	10	58[e]	14:1	87

Reaction conditions: [a]THF, 40 °C; [b,c]NaOCl, DCM, 4-phenylpyridine *N*-oxide ([b]20 mol %, [c]40 mol %), rt. [d]Crude epoxide yield ($\alpha + \beta$). [e]Isolated yields for **8α**. [f]Ratio calculated by NMR in the isolated crude mixture.

The oxepane scaffold was then ready for diversification via epoxide opening to generate functionalized oxepane nucleosides. The reaction of **8α** with 10 equiv of $LiEt_3BH$ at 0 °C resulted in a completely stereo- and regioselective conversion to **9** in 36% yield, together with unreacted starting material. Additional equivalents of $LiEt_3BH$ did not increase the yield of the reaction and resulted in formation of base reduction products. Regioselective opening of epoxide **8α** can be explained by the possible coordination of $LiEt_3BH$ to the nucleobase and directing the attack of hydride to the proximal and less hindered C3′ position. The regio- and stereochemistry of **9** was confirmed by COSY and NOESY NMR experiments, respectively. Cleavage of the silyl protecting group afforded nucleoside **10** in 87% yield (Scheme 2).

Scheme 2. Regio-/Stereoselective Synthesis of Oxepane Nucleoside 10

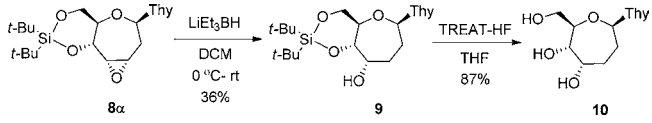

To further explore the scope of our strategy to synthesize structurally diverse oxepane nucleosides, diastereomerically pure **8α** was desilylated with TREAT-HF in 90% yield to afford epoxide **11** that was then reacted with NaN_3 in DMF at 100 °C and in the presence of 15-crown-5 (Scheme 3). Unlike the hydride reduction described above for protected nucleoside **8α**, the azidation reaction of **11** resulted in a 1:2.3 mixture of **13** and **14** in 70% combined yield. The regioselectivity and yield of this step dropped significantly when azidation was carried out on **8α** instead. The position of the azide group in both **13** and **14** regioisomers was determined by COSY NMR in DMSO-d_6. The configuration was assessed by NOESY experiments. A clear correlation between H6 of the nucleobase and H3′ was observed for compound **14**, suggesting the β configuration of H3′. In the case of regioisomer **13**, a correlation between H4′ and H6 was observed instead, suggesting a *cis* relative orientation between the thymine and H4′ (Scheme 3).

Interestingly, reaction of epoxide **11** with NaF/KHF_2 in ethylene glycol at 120 °C resulted in an isomerization to afford anhydro nucleoside **12** in high yield, as assessed by NMR and UV experiments. NaF/KHF_2 salts were found to not play a role in the isomerization, as heating **11** in the absence of fluoride afforded **12** in the same yield and reaction time. The identity, stereochemistry, and conformation of anhydro nucleoside **12** were unambiguously assigned by single-crystal X-ray diffraction. Within the bicyclic structure, the oxepane ring adopts a chairlike conformation in which the hydroxymethyl group and 5′-OH are equatorial, while the thymine base and the 4′-OH group are pseudoaxial (Scheme 3). We next turned our attention to chlorine functionalization, given the recent discovery of chlorinated nucleoside analogues with promising biological activity.[23,24] Indeed, reaction of **12** with HCl-Py in DMF provided the desired chlorinated nucleoside analogue **15** with complete stereoselectivity in 88% yield (Scheme 3).

DOI: 10.1021/acs.orglett.5b02769
Org. Lett. 2015, 17, 5416−5419

Scheme 3. Synthesis of Azido (13, 14) and Chloro (15) Oxepane Nucleosides[a]

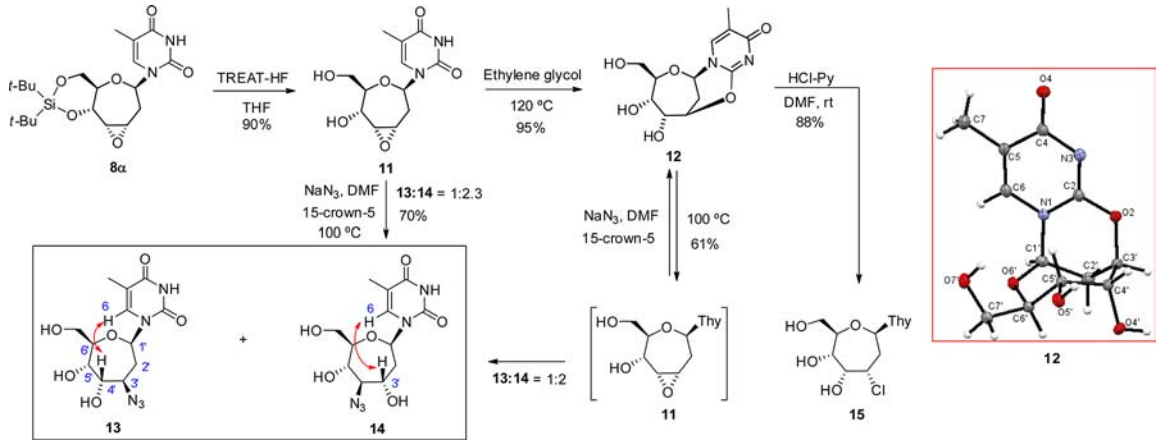

[a]Crystal structure of nucleoside **12** and key NOE correlations in **13** and **14**.

Interestingly, when **12** was subjected to azidation conditions, the expected product resulting from nucleophilic α-attack at the 3′-position was not detected. Instead, a regioisomeric mixture of compounds **13** and **14** was obtained in a ratio similar to that of azidation of epoxide **11**. As previously reported for furanose nucleosides,[25] we hypothesize that **12** equilibrates to epoxide **11** under these conditions, and that **11** is the direct precursor of **13** and **14** (Scheme 3). To further study the mechanism of this reaction, **12** was dissolved in DMF-d_6 in the absence of NaN_3 and crown ether. After being heated for 3 h at 100 °C in an NMR tube, no changes were observed in the ^{1}H NMR spectrum, suggesting that nucleophilic conditions are crucial in this case to drive the equilibrium toward epoxide **11**.

Conformational Analysis

With this new set of oxepane nucleosides in hand, we next embarked on the analysis of the structural properties of two of the analogues, **10** and **11**. The ring pucker of seven-membered ring systems can be described as a combination of boat/twist-boat (B/TB) and chair/twist-chair (C/TC) pseudorotational cycles.[26,27] The torsional landscape of **10** and **11** was first assessed by molecular dynamics simulations coupled to a metadynamics enhanced sampling scheme (see Supporting Information). The most stable conformations were further minimized using quantum mechanical density functional theory calculations at the M062X/6-31+G(d,p) level using MeOH as solvent (full details in Supporting Information). Our calculations show that lowest-energy states for epoxide **11** correspond to a chairlike conformation, in which all the substituents assume a pseudoequatorial disposition to alleviate steric interactions (Figure 2a). The differences in stability among the lowest-energy states are due to small variations in the orientation of the thymine and hydroxymethyl substituents; meanwhile, the sugar pucker remains almost invariable (details in Supporting Information). Lowest-energy states for the alcohol derivative **10** are mixtures of twisted chair and boat conformations (~65 and ~35%, respectively) (Figure 2b). The main differences among low-energy states are also in this case due to small variations in the orientation of the substituents, causing very minor variations in the sugar conformation (Supporting Information).

Calculated $^3J_{HH}$ values based on the Boltzmann distribution of the computed low-energy conformers of **10** and **11** were compared with experimental $^3J_{HH}$ values from ^{1}H NMR coupling constant analysis in MeOH-d_4 (Table 2; details in Supporting Information). For **11**, there was sufficient spectral resolution of all the resonances so that coupling constants could be conveniently extracted from the spectra. In the case of **10**, the large number of couplings involved in H2′ and H3′ protons prevented the extraction of the coupling constants between these

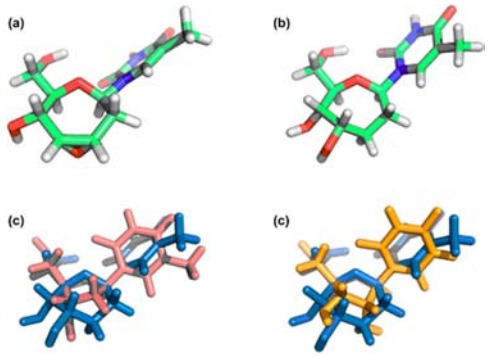

Figure 2. Lowest-energy conformations of (a) **11** and (b) **10**. Derivative **10** is a mixture of boat and twisted boat conformations, and **11** is found exclusively in the chair conformation. Superposition of **10** (blue) with (c) C2′-*endo*-thymidine (red) and (d) C3′-*endo*-uridine (orange).

Table 2. Calculated and Experimental $^3J_{H,H}$ Coupling Constants (±0.2 Hz) for 10 and 11

coupling constant	calcd **10**[a]	exptl **10**[b]	calcd **11**[a]	exptl **11**[b]
$^3J_{1',2'}$	11.0	10.0	10.1	10.5
$^3J_{1',2''}$	2.3	3.4	0.7	2.4
$^3J_{2',3'}$	1.7		0.3	0
$^3J_{2'',3'}$	12.3		5.7	4.5
$^3J_{2',3''}$	6.0		NA	NA
$^3J_{2'',3''}$	2.5		NA	NA
$^3J_{3'',4'}$	1.0	2.0	NA	NA
$^3J_{3',4'}$	9.9	9.8	4.0	4.7
$^3J_{4',5'}$	4.2	2.5	0.6	0
$^3J_{5',6'}$	7.9	5.7	9.1	9.6

[a]Values calculated using GIAO/B3LYP/aug-cc-pVDZ methodology on optimized structures, averaged based on their Boltzmann population. [b]Observed coupling constants from ^{1}H NMR experiments in MeOH-d_4.

DOI: 10.1021/acs.orglett.5b02769
Org. Lett. 2015, 17, 5416−5419

protons. In general, there was good correspondence between calculated and observed $^3J_{HH}$, supporting the accuracy of the conformations provided by computation. The H1′ splitting pattern in both **10** and **11** are consistent with the pseudoequatorial orientation of the pyrimidine base. Figure 2c,d compares the 3D structure of compound **10** to the natural nucleosides (dT and rU) by superposition of the structures. When the bases are aligned, the pseudoequatorial C4′−OH bond in **10** superimposes rather well with the pseudoequatorial C3′−OH bond of uridine (shown in the favored C3′-*endo* conformation), suggesting that 4′,7′-linked oligomers of **10** may conform to the structure of natural nucleic acids (e.g., RNA).

In summary, we have described the synthesis of several novel oxepane nucleosides by using a diastereomerically pure epoxide as a common intermediate. Theoretical calculations and NMR studies suggest that these analogues adopt a chair conformation with the pyrimidine base in the equatorial orientation. We expect this new series of ring-expanded nucleic acid analogues to be useful as building blocks in the design of new functional genetic systems and gene silencing oligonucleotides.

■ ASSOCIATED CONTENT

Supporting Information

The Supporting Information is available free of charge on the ACS Publications website at DOI: 10.1021/acs.orglett.5b02769.

General methods, experimental procedures, full spectroscopic data, summary of energies, geometries, and details of classical and quantum mechanical calculations for each conformer of nucleosides **10** and **11** (PDF)
Crystallographic information for **12** (CIF)

■ AUTHOR INFORMATION

Corresponding Author

*E-mail: masad.damha@mcgill.ca.

Notes

The authors declare no competing financial interest.

■ ACKNOWLEDGMENTS

The authors thank Prof. D. Cremer (Southern Methodist University) for making his code for puckering calculations available to us. Financial support was provided by Discovery Grant from the Natural Sciences and Engineering Research Council of Canada (M.J.D.), the McGill CIHR Drug Development Training Program (M.H. and S.M-M.). This work was also supported by the European Union's Horizon 2020 research and innovation program under a Marie Sklodowska-Curie grant (654812 to G.P.), the Spanish National Institute of Bioinformatics (INB) (to M.O.), and the European Research Council (ERC) (Advanced Investigator grant to M.O.)

■ REFERENCES

(1) Sofia, M. J. *Annu. Rep. Med. Chem.* **2014**, *49*, 221−247.
(2) Parker, W. B. *Chem. Rev.* **2009**, *109*, 2880−2893.
(3) Marquez, V. E.; Ben-Kasus, T.; Barchi, J. J.; Green, K. M.; Nicklaus, M. C.; Agbaria, R. *J. Am. Chem. Soc.* **2004**, *126*, 543−549.
(4) Marquez, V. E.; Ezzitouni, A.; Russ, P.; Siddiqui, M. A.; Ford, H.; Feldman, R. J.; Mitsuya, H.; George, C.; Barchi, J. J. *J. Am. Chem. Soc.* **1998**, *120*, 2780−2789.
(5) Pitsch, S.; Wendeborn, S.; Jaun, B.; Eschenmoser, A. *Helv. Chim. Acta* **1993**, *76*, 2161−2183.
(6) Eschenmoser, A.; Dobler, M. *Helv. Chim. Acta* **1992**, *75*, 218−259.
(7) Verheggen, I.; Van Aerschot, A.; Toppet, S.; Snoeck, R.; Janssen, G.; Balzarini, J.; De Clercq, E.; Herdewijn, P. *J. Med. Chem.* **1993**, *36*, 2033−2040.
(8) Aerschot Van, A.; Verheggen, I.; Hendrix, C.; Herdewijn, P. *Angew. Chem., Int. Ed. Engl.* **1995**, *34*, 1338−1339.
(9) Taylor, A. I.; Pinheiro, V. B.; Smola, M. J.; Morgunov, A. S.; Peak-Chew, S.; Cozens, C.; Weeks, K. M.; Herdewijn, P.; Holliger, P. *Nature* **2015**, *518*, 427−430.
(10) Kanojia, R. M.; Wachter, M. P.; Levine, S. D.; Adams, R. E.; Chen, R.; Chin, E.; Cotter, M. L.; Hirsch, A. F.; Huettemann, R. *J. Org. Chem.* **1982**, *47*, 1310−1319.
(11) Basu, S.; Ellinger, B.; Rizzo, S.; Deraeve, C.; Schürmann, M.; Preut, H.; Arndt, H.-D.; Waldmann, H. *Proc. Natl. Acad. Sci. U. S. A.* **2011**, *108*, 6805−6810.
(12) Berger, D.; Overman, L. E.; Renhowe, P. A. *J. Am. Chem. Soc.* **1993**, *115*, 9305−9306.
(13) Basu, S.; Waldmann, H. *Bioorg. Med. Chem.* **2014**, *22*, 4430−4444.
(14) Sabatino, D.; Damha, M. J. *J. Am. Chem. Soc.* **2007**, *129*, 8259−8270.
(15) Castro, S.; Cherney, E. C.; Snyder, N. L.; Peczuh, M. W. *Carbohydr. Res.* **2007**, *342*, 1366−1372.
(16) Sizun, G.; Dukhan, D.; Griffon, J.-F.; Griffe, L.; Meillon, J.-C.; Leroy, F.; Storer, R.; Sommadossi, J.-P.; Gosselin, G. *Carbohydr. Res.* **2009**, *344*, 448−453.
(17) Tripathi, S.; Roy, B. G.; Drew, M. G. B.; Achari, B.; Mandal, S. B. *J. Org. Chem.* **2007**, *72*, 7427−7430.
(18) Nomura, M.; Endo, K.; Shuto, S.; Matsuda, A. *Tetrahedron* **1999**, *55*, 14847−14854.
(19) Abou Assi, H.; Martínez-Montero, S.; Dixit, D. M.; Chua, Z.; Bohle, D. S.; Damha, M. J. *Eur. J. Org. Chem.* **2015**, *2015*, 1945−1953.
(20) Deleavey, G. F.; Damha, M. J. *Chem. Biol.* **2012**, *19*, 937−954.
(21) Hoberg, J. O. *J. Org. Chem.* **1997**, *62*, 6615−6618.
(22) Itoh, T.; Jitsukawa, K.; Kaneda, K.; Teranishi, S. *J. Am. Chem. Soc.* **1979**, *101*, 159−169.
(23) Srivastav, N. C.; Shakya, N.; Mak, M.; Liang, C.; Tyrrell, D. L. J.; Agrawal, B.; Kumar, R. *Bioorg. Med. Chem.* **2010**, *18*, 7542−7547.
(24) Srivastav, N. C.; Shakya, N.; Bhavanam, S.; Agrawal, A.; Tse, C.; Desroches, N.; Kunimoto, D. Y.; Kumar, R. *Bioorg. Med. Chem. Lett.* **2012**, *22*, 1091−1094.
(25) Al-Masoudi, N. A.; Pfleiderer, W. *Carbohydr. Res.* **1995**, *275*, 95−105.
(26) Jahn, M. K.; Dewald, D. A.; Vallejo-López, M.; Cocinero, E. J.; Lesarri, A.; Zou, W.; Cremer, D.; Grabow, J.-U. *Chem. - Eur. J.* **2014**, *20*, 14084−14089.
(27) DeMatteo, M. P.; Snyder, N. L.; Morton, M.; Baldisseri, D. M.; Hadad, C. M.; Peczuh, M. W. *J. Org. Chem.* **2005**, *70*, 24−38.

DOI: 10.1021/acs.orglett.5b02769
Org. Lett. 2015, 17, 5416−5419